

Generation and characterization of customized perfect Laguerre-Gaussian beams with arbitrary profiles

Yun Chen,^{1,2} Chengyuan Wang,^{1,2,*} Xin Yang,^{1,†} Zehao Shen,¹ Wei Zhang,¹ Hong Gao,¹ and Fuli Li¹

¹*Ministry of Education Key Laboratory for Nonequilibrium Synthesis and Modulation of Condensed Matter, Shaanxi Province Key Laboratory of Quantum Information and Quantum Optoelectronic Devices, School of Physics, Xi'an Jiaotong University, Xi'an 710049, China*

²*Two authors have equal contributions on this work.*

We experimentally demonstrate the generation of customized perfect Laguerre-Gaussian (PLG) beams whose intensity maxima localized around any desired curves. The principle is to act appropriate algebraic functions on the angular spectra of PLG beams. We characterize the propagation properties of these beams and compare them with non-diffraction caustic beams possessing the same intensity profiles. The results manifest that the customized-PLG beams can maintain their profiles during propagation and suffer less energy loss than the non-diffraction caustic beams, and hence are able to propagate a longer distance. This new structure beam would have potential applications in areas such as optical communication, soliton routing and steering, optical tweezing and trapping, atom optics, etc.

I. INTRODUCTION

Structure lights with customized intensity, phase, and polarization distributions [1, 2] have promoted the development of fundamental physics [3], optical tweezers [4], imaging [5], optical communications [6], and light-matter interactions [7, 8], etc. Hermite-Gaussian (HG) beam [9, 10], Laguerre-Gaussian (LG) beam [11], and Ince-Gaussian beam [12, 13] are three representative structure lights, which are the solutions of the paraxial wave equation (PWE) under Cartesian, polar, and elliptical coordinates, respectively. These beams can remain their transverse profiles unchanged for about one Rayleigh length propagation, but their beam sizes would expand due to diffraction. In 1987, J. Durnin *et al.* propose that the zeroth-order Bessel beam possesses the non-diffraction characteristic [14], that is their transverse structures neither deform nor expand over a significant propagation distance. This kind of beam displays a highly localized concentric ring structure, which is similar to the LG modes [15]. However, a Bessel beam theoretically has infinite ring numbers and each ring carries equal energy, meaning that a Bessel beam has infinite energy and is inaccessible practically. So in experiment, the Bessel beams are apodized, e.g., by a Gaussian transmittance [16] and can propagate up to a finite distance without obvious diffraction. Recently, researchers make use of the formal connection between Bessel beams and LG beams (i.e., the relationship between the radial wave number of Bessel beam and the beam waist of LG beam) to propose a new spatial structure beam in theory, referred to as the perfect Laguerre-Gaussian (PLG) beam [17], and it was later verified experimentally [18]. The most striking difference between the PLG beam and the LG beam is that its outer ring's radius is independent of

the topological charge.

The structure beams mentioned above have specific optical field expressions and transverse intensity distributions. In some applications such as bio-particle transportation, atom trapping and manipulation, and soliton routing and steering, light beams with intensities concentrated along arbitrary desired trajectories would be more useful. However, structure beams (e.g., optical images) obtained through simple amplitude modulation by optical instruments are susceptible to diffraction and can not preserve their spatial profiles during propagation. To overcome this, researchers propose some methods to generate quasi-non-diffraction beams via spatial spectrum engineering techniques assisted with some optimization algorithms such as genetic algorithm [19], iterative Fourier algorithm [20, 21], differential evolution algorithm [22]. In 2020, A. Zannotti *et al.* construct arbitrary non-diffraction caustic beams through amplitude and phase modulation of the Bessel beam in Fourier space [23]. This beam can propagate a Rayleigh length while keeping its shape and size basically unchanged. Recently, J. Mendoza-Hernández theoretically proposes that by acting an algebraic function on a PLG beam in Fourier space, a new structure beam similar to the non-diffraction beam can also be generated [24]. It's demonstrated that such a beam can preserve their profiles a longer propagation distance than the non-diffraction beam. Nevertheless, this work doesn't extend to generating arbitrarily shaped beams and yearning for experimental realization.

In this paper, we experimentally generate customized-PLG beams with any desired shapes. The rationale is based on tailoring the PLG beams in Fourier space by algebraic functions [24–26], which are constructed using the methods in Ref. [23]. To assess the propagation properties of the customized-PLG beams, we also generate non-diffraction caustic (or customized-Bessel) beams [23] with the same transverse profiles for peer comparison. The experimental results show that the customized-PLG

* wcy199202@gmail.com

† xinyang@xjtu.edu.cn

beams can maintain their profiles during propagation and suffer less energy loss than the customized-Bessel beams, and hence can propagate a longer distance.

II. THEORETICAL DESCRIPTION

When a linear differential operator $\hat{\mathcal{A}}$ acts on an appropriate seed beam $U_0(r, z)$, a new beam $U(\mathbf{r}, z)$ can be obtained with an arbitrary desired shape [24, 25]. Such a transformation process can be expressed as

$$U(\mathbf{r}, z) = \hat{\mathcal{A}}U_0(r, z), \quad (1)$$

where $\mathbf{r} = (x, y)$ is the transverse coordinate. Using the Fourier transform \mathcal{F} and inverse Fourier transform \mathcal{F}^{-1} , Eq. (1) can be further written as

$$U = \mathcal{F}^{-1} \left\{ \mathcal{F} \left\{ \hat{\mathcal{A}}U_0 \right\} \right\} = \mathcal{F}^{-1} \left\{ \mathcal{A} \mathcal{F} \{U_0\} \right\} = \mathcal{F}^{-1} \left\{ \mathcal{A}\tilde{U}_0 \right\}, \quad (2)$$

where \mathcal{A} is an algebraic function corresponding to the operator $\hat{\mathcal{A}}$ in Fourier space [25], \tilde{U}_0 is the Fourier transform of U_0 .

In this paper, we consider the two cases of seed beam: 0th-order Bessel beam and PLG beam. The seed-Bessel beam in Fourier space is a thin ring, which is defined as

$$B\tilde{U}_0 = \delta(r - r_b) \quad (3)$$

where $\delta(r - r_b)$ is the delta function with ring radius r_b (its ring width Δr_b is infinitesimal).

The seed-PLG beam, used to produce the PLG beam and its derived structured light field, is defined as

$$PLG\tilde{U}_0 = CL_p^{[0]} \left(\frac{2r^2}{\omega_{kt}^2(0)} \right) \exp \left[-\frac{r^2}{\omega_{kt}^2(0)} \right] \quad (4)$$

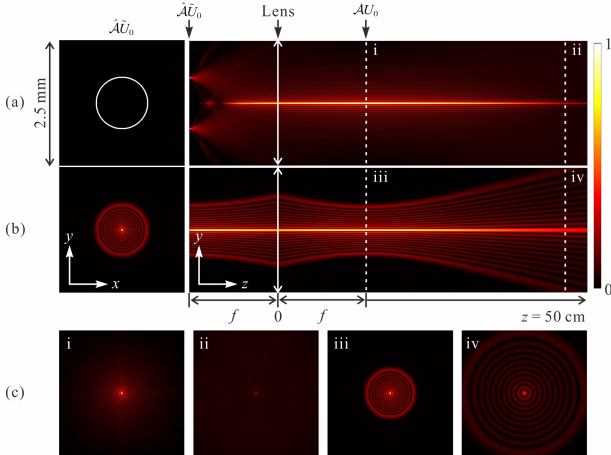


FIG. 1. Theoretical simulation of the generation and propagation of (a) Bessel beam and (b) PLG beam. (c) Intensity profiles of the two beams at $z = 0$ and $z = 45$ cm. The parameters used in the simulations are $r_b = 1$ mm, $\Delta r_b = 50$ μ m for the Bessel beam, and $\omega_0 = 2.1$ mm, $p = 10$ for the PLG beam, the focal length of the lens $f = 200$ mm, the wavelength of light $\lambda = 780$ nm.

where C is a constant coefficient, $L_p^{[0]}$ is the Laguerre polynomial with the radial order p and azimuthal order $l = 0$, $\omega_{kt}(0) = \omega_0/2\sqrt{2N}$ with the input Gaussian beam waist ω_0 and $N = p + (|l| + 1)/2$.

In the simplest case, namely acting $\mathcal{A} = 1$ on $B\tilde{U}_0$ or $PLG\tilde{U}_0$ and takes the inverse Fourier transform by a lens, a Bessel or PLG beam is generated. Figure 1 shows the theoretical simulation of this conversion process (the relevant parameters are given in the caption). The first columns of Fig. 1(a) and 1(b) are the transverse structures of $B\tilde{U}_0$ and $PLG\tilde{U}_0$, and the second columns are the beams' propagation trajectories. The images *i* and *iii* in Fig. 1(c) are the Bessel and PLG beams obtained at the focal plane of the converging lens, while images *ii* and *iv* present their transverse intensity profiles at a propagation distance of 45 cm. As can be seen that the Bessel beam maintains its overall profile during propagation but its intensity attenuates fastly whereas the PLG beam can maintain its intensity profile much better but suffer a little broadening.

To produce diverse shaped beams, we can select or construct more complicated \mathcal{A} . Figure 2(a) and 2(b) give two examples of designed astroid and deltoid distributions when the algebraic functions are selected as $\mathcal{A}_A = \exp[i(l\varphi + q_A \sin(2\varphi))]$ and $\mathcal{A}_D = \exp[iq_D \sin^3(\varphi)]$ [23]. Here φ is the azimuthal angle in spatial-frequency domain, q_A and q_D are constants. The first columns show the angular spectra corresponding to $\mathcal{A}_{A/D}B\tilde{U}_0$ and $\mathcal{A}_{A/D}PLG\tilde{U}_0$, the second columns and the third columns are the intensities $|U_0|$ and the phase distributions $\text{Arg}(U_0)$ of the customized beams. As we can see, under the set parameters, for the same algebraic function, the customized fields constructed by the two seed beams have very similar spatial structure, which ensures their comparability in propagation characteristics.

To generate more universal beams that have no explicit function forms, we adopt the 'Bessel-pencil' method [23] for reference to construct their algebraic functions. This method utilizes the most localized propagation-invariant light spot, namely a 0th-order Bessel beam, as a 'pencil' to draw the desired beam along a preset curve. The algebraic function of such a beam can be constructed by

$$\mathcal{A} = \int_a^b A_B(\tau) \exp[i\gamma_B(\tau) - ik_t \mathbf{r}_c(\tau) \cdot \mathbf{u}(\varphi)] d\tau \quad (5)$$

where $A_B(\tau)$ and $\gamma_B(\tau)$ are the amplitude and phase of \mathcal{A} , respectively, k_t is a variable parameter in the range from 0 to $2\pi/\lambda$ to determine the scale and details of the customized beam [27], $\mathbf{r}_c = (x_c, y_c)$ is the transverse coordinate along the desired curve, $\mathbf{u}(\varphi) = (\cos\varphi, \sin\varphi)$ is a unit vector, and τ is the arc length of the curve, and a/b is the head /tail of the curve. The phase term $\gamma_B(\tau)$ should grow with the curve's arc length τ , which can be obtained by

$$\gamma_B(\tau) = k_t \int_0^\tau |\mathbf{r}'_c(s)| ds \quad (6)$$

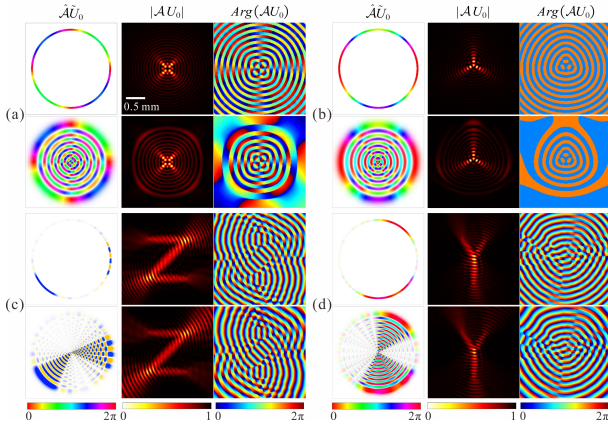


FIG. 2. (a) Theoretical simulation of customized Bessel beams and PLG beams with (a) astroid, (b) deltoid, (c) ‘Z’ shape, and (d) ‘Y’ shape. The first column is the angular spectrum ($\hat{A}\tilde{U}_0$), the second and third columns are the beam’s intensity distribution ($|U_0|$) and phase distribution ($Arg(U_0)$). The parameters used in the simulations are $r_b = 1$ mm, $\Delta r_b = 50$ μ m for the customized-Bessel beams, and $\omega_0 = 2.1$ mm, $l = 0$, $q_A = 0.4$, $q_D = 0.2$, $p = 10$ in (a) and (b), and $p = 20$ in (c) and (d) for the customized-PLG beams, $k_t = 2.66 \times 10^5 m^{-1}$.

We integrate Eq. (5) along two designed curves, i.e., a letter ‘Z’ and a letter ‘Y’, and obtain the corresponding algebraic functions \mathcal{A}_Z and \mathcal{A}_Y . Acting them on $B\tilde{U}_0$ and $PLG\tilde{U}_0$ respectively, we obtain four angular spectra, as shown in the first columns of Fig. 2(c) and 2(d). The second columns are the intensity distributions of the corresponding target beams, from which we can see that the beams’ intensity maxima indeed follow the shapes of the letters ‘Z’ and ‘Y’.

III. EXPERIMENTAL RESULTS AND DISCUSSIONS

In the following we experimentally generate several representative customized-PLG and customized-Bessel

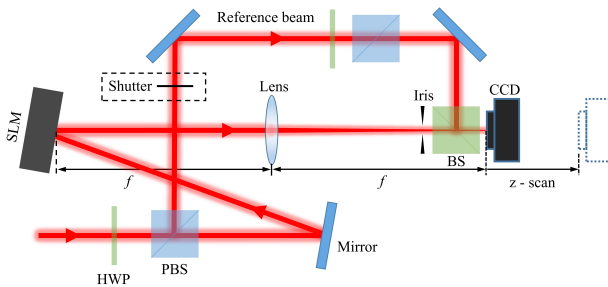


FIG. 3. (a) Experimental setup. HWP: half wave plate; PBS: polarization beam splitter; SLM: spatial light modulator with one pixel size of 12.5×12.5 μ m; BS: beam splitter; CCD: charge-coupled device.

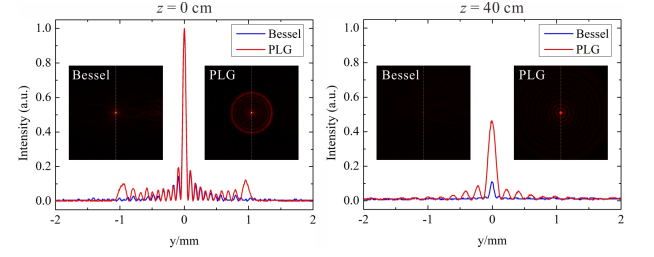


FIG. 4. Intensity profile comparison of the experimentally generated Bessel beam and PLG beam at a propagation distance of (a) $z = 0$ cm and (b) $z = 40$ cm.

beams based on the methods above. The experimental setup is illustrated in Fig. 3. A horizontally polarized Gaussian beam incident on a spatial light modulator (SLM) carried with a pre-calculated phase, and the reflected beam is modulated to the target $A\tilde{U}_0$. The desired beam can be obtained by inverse Fourier transform of $A\tilde{U}_0$ using a lens. A charge-coupled device (CCD) is placed at the focus of the lens to capture the beam’s transverse profile. The position of the CCD can also be shifted through a translation stage to record the revolution of the beam during its propagation. Besides, an additional reference beam can be switched on by a shutter to interference with the customized beams for phase measurements.

Firstly we let $\mathcal{A} = 1$ to generate a Bessel beam and a PLG beam (Fig. 4). The related parameters used in the experiment are $r_b = 1$ mm, $\Delta r_b = 50$ μ m, $\omega_0 = 2.1$ mm, $p=10$, and $f = 200$ mm, as in theory. The values of r_b and ω_0 ensure that the two types of beams have the same intensity distributions in the focal plane of the lens, as can be seen in Fig. 4(a). Theoretically smaller Δr_b enables a more ideal Bessel beam. But practically we set $\Delta r_b = 50$ μ m since it almost approaches the resolution of the SLM, and a smaller Δr_b will decrease the modulation quality and the generation efficiency of the target beam. Figure 4(b) shows the intensity distributions of the two beams after propagating a distance of 40 cm in free space. The Bessel beam depletes severely and its intensity maximum drops to 10%, while the PLG beam depletes much slower and its intensity maximum falls to 46%. Meanwhile, the side-lobes of the PLG beam are also more recognizable than that of the Bessel beam after propagation.

Next, we generate several complicated patterns, e.g., astroid, deltoid, ‘Z’-shaped, and ‘Y’-shaped beams, and record their intensity distributions after propagation distances of 0 cm, 20 cm, and 40 cm, as shown in Fig. 5, where (a), (c), (e), and (g) corresponds to the customized-Bessel beam and (b), (d), (f), and (h) corresponds to the customized-PLG beam. The related parameters are the same with Fig. 4 except for $p=20$ for (f) and (h). At $z = 0$, the central regions of both beams are tailored into the same desired shapes. The difference is that the customized-PLG beams’ outer rings are more

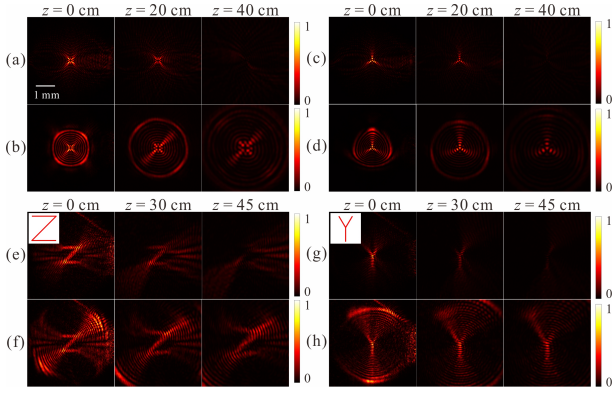


FIG. 5. Intensity profiles of the experimentally generated customized beams at different propagation distances. (a) and (b) astroid shape, (c) and (d) deltoid shape, (e) and (f) ‘Z’ shape, (g) and (h) ‘Y’ shape. (a), (c), (e), and (g) correspond to customized-Bessel, and (b), (d), (f), and (h) correspond to customized-PLG.

pronounced than that of the customized-Bessel beam. This is due to that the intensities of the PLG’s outer rings are higher, as can be seen in Fig. 1 and Fig. 4. During propagation, the customized-Bessel beams exhibit non-diffraction characteristics but their intensities decay dramatically and are almost invisible after a propagation distance of more than 40 cm. In contrast, the customized-PLG beams also maintain their overall shapes except for little deformations and expansions with the increase of the propagation distance, while their intensities deplete much slower and are still recognizable over 40 cm propagation distance. As can be seen from the above results that the propagation properties of customized beams follow that of the corresponding seed beams. This is due to that the customized beams could be considered as the coherent superposition of the seed beams [23].

The summation of each beam’s intensity in the central region around the desired curve in Fig. 5(e)-(h) is further calculated for quantitative comparison, as shown in Fig. 6. The corresponding theoretical simulations are also presented with solid lines. After propagating for 45 cm, the intensity of the ‘Z’-shaped customized-PLG beam attenuates to 72% of the original, while the intensity of the ‘Z’-shaped customized-Bessel beam only retains 27%. Similarly, the ‘Y’-shaped customized-PLG beam’s intensity is much higher than that of ‘Y’-shaped customized-Bessel beam under the same propagation distance.

Moreover, we use a reference beam to interfere with the customized beams and record the interference patterns, then apply the holographic interferometry method [28] to determine the phase distributions of the customized beams, as shown in the second and fourth columns of Fig. 7. The intensity profiles of the object beams are also reconstructed for comparison, as shown in the first and third columns of Fig. 7. All the results agree well with the theory, indicating that the generation qualities

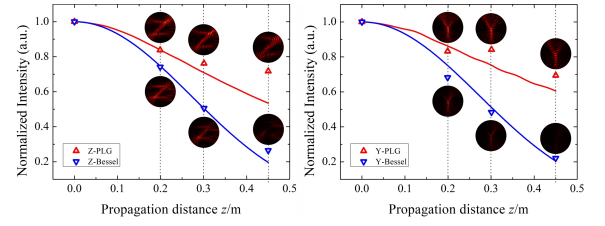


FIG. 6. Intensity variation of the customized-Bessel beam and customized-PLG beam with propagation distance. The red (blue) triangles are experimental results of customized-Bessel (customized-PLG) beam and the solid lines are the corresponding theoretical simulations.

of the customized beams are very well.

IV. CONCLUSION

In summary, we experimentally generate a series of customized-PLG beams that can present any desired high-intensity distributions. The key ingredient is based on tailoring the angular spectrum of the PLG beam by an algebraic function, which is constructed using the ‘Bessel-pencil’ method. We also generate some non-diffraction caustic beams that possess the same intensity profiles with the customized-PLG beams for comparison. The results show that the customized-PLG beams can maintain their profiles and suffer less energy loss than the non-diffraction caustic beams and hence can propagate a longer distance. The phase structures of all the generated beams are also determined by the holographic interferometry method, which agrees well with the theory and further validates the generation quality of the customized beams. This new phyletic structure beam could find broad applications in areas such as optical communication, spatial soliton control, optical tweezing and trap-

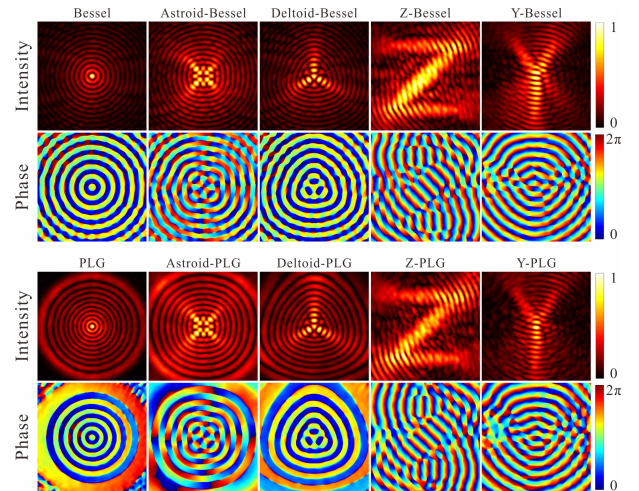


FIG. 7. Experimentally measured transverse intensities and phases of different beams.

ping, atom optics, etc.

11534008, 12033007, and 61875205).

FUNDING

This work is supported by National Natural Science Foundation of China (NSFC) (12104358, 92050103,

-
- [1] H. Rubinsztein-Dunlop, A. Forbes, M. V. Berry, M. R. Dennis, D. L. Andrews, M. Mansuripur, C. Denz, C. Alpmann, P. Banzer, T. Bauer, *et al.*, *J. Opt.* **19**, 013001 (2016).
 - [2] A. Forbes, M. de Oliveira, and M. R. Dennis, *Nat. Photonics* **15**, 253 (2021).
 - [3] A. Hansen, J. T. Schultz, and N. P. Bigelow, *Optica* **3**, 355 (2016).
 - [4] J. Baumgartl, M. Mazilu, and K. Dholakia, *Nat. photonics* **2**, 675 (2008).
 - [5] T. Vettenburg, H. I. Dalgarno, J. Nylk, C. Coll-Lladó, D. E. Ferrier, T. Čížmár, F. J. Gunn-Moore, and K. Dholakia, *Nat. methods* **11**, 541 (2014).
 - [6] J. P. Torres, *Nat. Photonics* **6**, 420 (2012).
 - [7] C. Wang, Y. Yu, Y. Chen, M. Cao, J. Wang, X. Yang, S. Qiu, D. Wei, H. Gao, and F. Li, *Quantum Sci. Technol.* **6**, 045008 (2021).
 - [8] Y. Chen, J. Wang, C. Wang, S. Zhang, M. Cao, S. Franke-Arnold, H. Gao, and F. Li, *Opt. Express* **29**, 31582 (2021).
 - [9] E. G. Abramochkin and V. G. Volostnikov, *Phys. Wave Phen.* **18**, 14 (2010).
 - [10] Y. Wang, Y. Chen, Y. Zhang, H. Chen, and S. Yu, *J. Opt.* **18**, 055001 (2016).
 - [11] L. Allen, M. Padgett, and M. Babiker, *Progress in optics* **39**, 291 (1999).
 - [12] M. A. Bandres and J. C. Gutiérrez-Vega, *Opt. Lett.* **29**, 144 (2004).
 - [13] Y. Yu, Y. Chen, C. Wang, J. Wang, Z. Sun, M. Cao, H. Gao, and F. Li, *Opt. Lett.* **46**, 1021 (2021).
 - [14] J. Durnin, J. J. Miceli, and J. H. Eberly, *Phys. Rev. Lett.* **58**, 1499 (1987).
 - [15] J. Mendoza-Hernández, M. L. Arroyo-Carrasco, M. D. Iturbe-Castillo, and S. Chávez-Cerda, *Opt. Lett.* **40**, 3739 (2015).
 - [16] J. C. Gutiérrez-Vega and M. A. Bandres, *JOSA A* **22**, 289 (2005).
 - [17] J. Mendoza-Hernández, M. Hidalgo-Aguirre, A. I. Ladino, and D. Lopez-Mago, *Opt. Lett.* **45**, 5197 (2020).
 - [18] X. Liu, Y. E. Monfared, R. Pan, P. Ma, Y. Cai, and C. Liang, *Appl. Phys. Lett.* **119**, 021105 (2021).
 - [19] P. A. Sanchez-Serrano, D. Wong-Campos, S. Lopez-Aguayo, and J. C. Gutiérrez-Vega, *Opt. Lett.* **37**, 5040 (2012).
 - [20] S. López-Aguayo, Y. V. Kartashov, V. A. Vysloukh, and L. Torner, *Phys. Rev. Lett.* **105**, 013902 (2010).
 - [21] C. Wang, Y. Chen, Z. Jiang, Y. Yu, M. Cao, D. Wei, H. Gao, and F. Li, *Front. Phys.* **17**, 1 (2022).
 - [22] A. F. Martínez-Herrera, A. Céspedes-Mota, and S. Lopez-Aguayo, *J. Opt. Soc. Am. A* **36**, 1968 (2019).
 - [23] A. Zannotti, C. Denz, M. A. Alonso, and M. R. Dennis, *Nat. Commun.* **11**, 3597 (2020).
 - [24] J. Mendoza-Hernández, *Opt. Lett.* **46**, 5232 (2021).
 - [25] I. Martinez-Castellanos and J. C. Gutiérrez-Vega, *Opt. Lett.* **40**, 1764 (2015).
 - [26] J. Mendoza-Hernández, M. Szatkowski, M. F. Ferrer-Garcia, J. C. Gutiérrez-Vega, and D. Lopez-Mago, *Opt. Express* **27**, 26155 (2019).
 - [27] J. Durnin, *J. Opt. Soc. Am. A* **4**, 651 (1987).
 - [28] G. T. Nehmetallah, R. Aylo, and L. Williams, *Analog and Digital Holography with MATLAB* (SPIE, 2015).

Appendix A: Influence of the radial index p on the propagation property of customized PLG beam

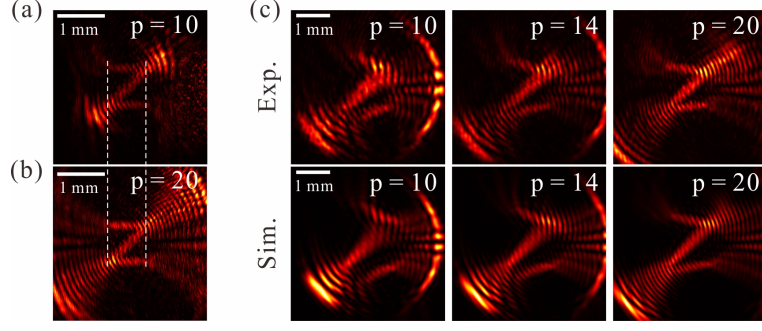


FIG. 8. Influence of the radial index p on the propagation property of customized PLG beam. (a) and (b) The beams' intensity profiles for $p = 10$ and $p = 20$ at $z = 0$. (c) The beam's intensity profile for $p = 10$, $p = 14$, and $p = 20$ at $z = 35$ cm. The first and the second columns are the experimental results and the theoretical simulations, respectively.

The beam waist of a seed-PLG in Eq. 4 is $\omega_{kt}(0) = \omega_0 / \sqrt{8p + 4|l| + 4}$. After Fourier transformed by a lens, the beam waist of the corresponding PLG beam ($\omega_{PLG}(0)$) is inversely proportional to $\omega_{kt}(0)$. The perfect diffraction distance L_D of this PLG beam satisfies $L_D \propto \omega_{PLG}^2(0)$ [17]. Hence for a given ω_0 and $|l|$, the larger the radial index p , the longer the propagation distance of the PLG beam. As we have mentioned in the manuscript, the customized-PLG beam inherits the spatial structure characteristic as well as the propagation property of the PLG beam. Therefore a large p is a prerequisite for the shape-preserving propagation of the customized-PLG beam. Meanwhile, large p would bring more 'sidebands' to the customized-PLG beam without changing the desired high-intensity curve contained therein (see Fig. 8(a) and 8(b)). In Fig. 8(c), the intensity profiles of 'z'-shaped PLG beams for $p = 10$, $p = 14$, and $p = 20$ at a propagation distance of 35 cm are shown for comparison, it's clearly that the larger the p , the better the shape preservation of the beam.